

A Comparison of Human Physical Models Used in the ISO 10068:2012 Standard Based on Power Distribution PART 1

Marian Witalis DOBRY

Poznan University of Technology, Institute of Applied Mechanics
24 Jana Pawła II Street, 60-965 Poznan
marian.dobry@put.poznan.pl

Tomasz HERMANN

Poznan University of Technology, Institute of Applied Mechanics
24 Jana Pawła II Street, 60-965 Poznan
tomasz.hermann@put.poznan.pl

Abstract

The study analyses differences in the flow of energy for two human physical models specified in the ISO 10068:2012 standard. For this purpose, two mathematical models of the Human–Tool system in question were developed using the Lagrange equation of the second kind. Corresponding energy models were then created for each mathematical model and tested by means of digital simulation in the MATLAB/simulink environment. The study revealed a discrepancy between the models in terms of different types of power and in the total power.

Keywords: biomechanical system, local vibrations, power distribution

1. Introduction

Biomechanical models of the hand and the hand–arm system are effectively used to represent the human response to mechanical vibrations. At present, the impact of vibrations can be studied based on any of the existing models, which differ in the number of degrees of freedom, the number of component parts of the dynamic structure and the manner in which they are connected (Fig. 1).

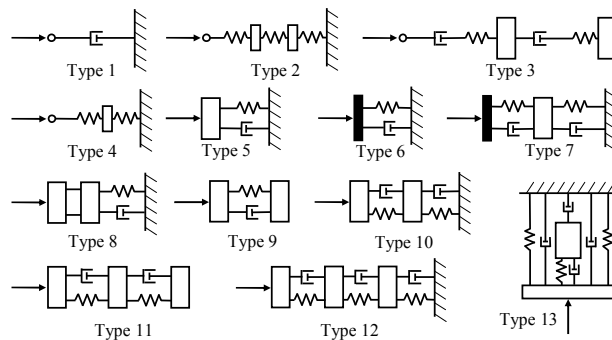


Figure 1. Biomechanical models of the hand and the hand–arm system [6]

One area that requires further research is the composition and verification of new models which are being developed to replace previous models and better represent the human response to mechanical vibrations. This kind of research is being conducted all over the world, including influential contributions from Griffin [5], Reynolds [8] and Meltzer [7].

To date, many studies into the impact of vibrations on the human body have relied on the “Type 12” model (Fig. 1), whose dynamic parameters are specified in the ISO 10068:1998 standard [9]. The fact that this long-favoured solution is being abandoned confirms that choosing the right model to assess the impact of vibrations on the human body is not an easy task. This study is an attempt at comparing power distribution in two biomechanical models of the human body, which are specified in the ISO 10068:2012 standard [10] – models 1 and 2 (Annexes B and C). The criterion for assessing model validity was the equality of energy phenomena occurring the dynamic structure during operation.

2. The First Principle of Power Distribution in a Mechanical System

The First Principle of Power Distribution in a Mechanical System can be expressed in the following way [1 – 4]:

„The net input power introduced into the mechanical system (after subtracting power loss) is equal to reflected power (accumulated or stored) in the system and output power from the system.”

A graphical interpretation of the First Principle of Power Distribution in a Mechanical System (FPoPDiMS) is shown in Figure 2.

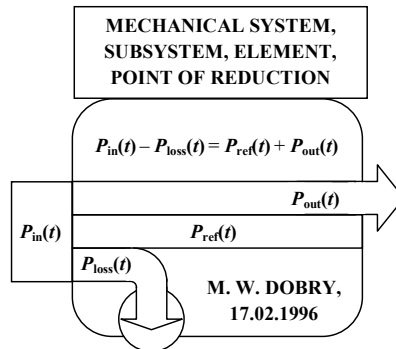


Figure 2. Graphical interpretation of the First Principle of Power Distribution [1-4]

This rule has the following mathematical form [1-4]:

$$P_{in}(t) - P_{loss}(t) = P_{ref}(t) + P_{out}(t) \quad (1)$$

where:

$$P_{in}(t) = \vec{W}_{in}(t) \cdot \vec{v}_{in}(t)$$

– the power of the resultant force – the drive input power introduced to the mechanical system,

- $P_{\text{loss}}(t) = P_{\text{int loss}}(t) + \vec{R}(t) \cdot \vec{v}_R(t)$ – power loss equal to the sum of the internal losses in the system and the power of the forces of resistance present during the operation of the system,
- $P_{\text{ref}}(t) = \vec{B}(t) \cdot \vec{v}_B(t) + \vec{S}(t) \cdot \vec{v}_S(t)$ – reflected power in the mechanical system, equal to the sum of inertial forces and the power of the forces of elasticity,
- $P_{\text{out}}(t) = \vec{O}(t) \cdot \vec{v}_{\text{out}}(t)$ – output power equal to the power output of a mechanical system.

3. The methodology of solving the problem – composition of energy models

To conduct a comparative assessment of the two models it was necessary to create physical models of the Human–Tool system. These models are the result of combing the human physical models specified in the ISO 10068:2012 standard [10] with the tool model – Fig. 3.

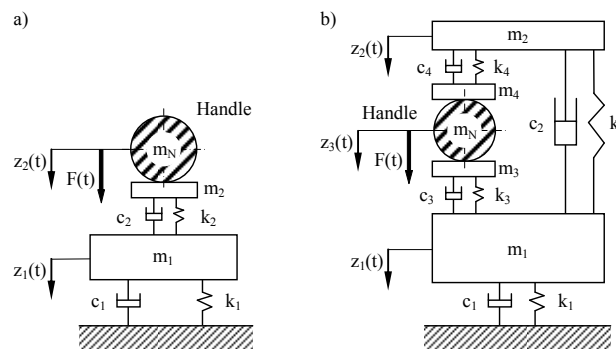


Figure 3. A synthesis of the ISO 10068:2012-based human physical models and the tool model: a) model 1 – Annex B; b) model 2 – Annex C [10]

The models in question are discrete in the sense that certain reduction points are connected by means of spring and damping systems. Tables 1 and 2 present dynamic parameters for the models, as indicated in the ISO 10068:2012 standard [10]. In the dynamic analysis only one vibration direction was considered – the z direction, which is the most significant in tool testing

The next step involved expressing the mathematical models of the dynamic structures using the Lagrange equation of the second kind in the following form:

$$\frac{d}{dt} \left(\frac{\partial E}{\partial \dot{q}_j} \right) - \frac{\partial E}{\partial q_j} = Q_j + Q_{jP} + Q_{jR} \quad j = 1, 2, \dots, s \quad (2)$$

where: E – kinetic energy of the system, q_j – generalized coordinates, \dot{q}_j – generalized velocities, Q_j – external active forces, Q_{jP} – potential forces, Q_{jR} – dissipation forces, s – number of degrees of freedom.

Table 1. Values of dynamic parameters for model 1 – Annex B [10]

Parameter	Unit	Vibration direction		
		x	y	z
m_1	kg	0.5479	0.5374	1.2458
m_2	kg	0.0391	0.0100	0.0742
k_1	N/m	400	400	1000
k_2	N/m	0	17648	50000
c_1	N·s/m	22.5	38.3	108.1
c_2	N·s/m	202.6	75.5	142.4

Table 2. Values of dynamic parameters for model 2 – Annex C [10]

Parameter	Unit	Vibration direction		
		x	y	z
m_1	kg	0.4129	0.7600	1.1252
m_2	kg	0.0736	0.0521	0.0769
m_3	kg	0.0163	0.0060	0.0200
m_4	kg	0.0100	0.0028	0.0100
k_1	N/m	400	500	1000
k_2	N/m	200	100	12000
k_3	N/m	4000	4907	43635
k_4	N/m	8000	17943	174542
c_1	N·s/m	20.0	28.1	111.5
c_2	N·s/m	100	39.7	39.3
c_3	N·s/m	144.6	50.7	86.8
c_4	N·s/m	79.9	14.3	121.0

For an unequivocal description generalized coordinates were adopted. For model 1 from the ISO 10068:2012 standard [10], the following generalized coordinates were used (Fig. 3a):

$$\begin{aligned} j=1 & \Rightarrow q_1 = z_1(t) && \text{– displacement of mass } m_1, \\ j=2 & \Rightarrow q_2 = z_2(t) && \text{– displacement of mass } m_2 \text{ and } m_N. \end{aligned}$$

In the case of model 2 from the ISO 10068:2012 standard [10] combined with the tool model (Fig. 3b), the following generalized coordinates were used:

$$\begin{aligned} j=1 & \Rightarrow q_1 = z_1(t) && \text{– displacement of mass } m_1, \\ j=2 & \Rightarrow q_2 = z_2(t) && \text{– displacement of mass } m_2, \\ j=3 & \Rightarrow q_3 = z_3(t) && \text{– displacement of mass } m_3, m_4 \text{ and } m_N. \end{aligned}$$

On adopting generalized coordinates, it was possible to formulate mathematical models of the Human–Tool system. For the Human–Tool system (ISO 10068:2012 combined with model 1 [10]) the mathematical model can be expressed as – Fig. 3a:

$$\begin{aligned} j=1, & \quad m_1 \ddot{z}_1 + (c_1 + c_2) \dot{z}_1 + (k_1 + k_2) z_1 - c_2 \dot{z}_2 - k_2 z_2 = 0; \\ j=2, & \quad (m_2 + m_N) \ddot{z}_2 + c_2 \dot{z}_2 + k_2 z_2 - c_2 \dot{z}_1 - k_2 z_1 = F(t). \end{aligned} \quad (3)$$

The mathematical model of the synthesis of the ISO 10068:2012-based model 2 [10] with the tool model – Fig. 3b, can be written as:

$$\begin{aligned}
j = 1, & \quad m_1 \ddot{z}_1 + (c_1 + c_2 + c_3) \dot{z}_1 + (k_1 + k_2 + k_3) z_1 - c_3 \dot{z}_3 - k_3 z_3 - c_2 \dot{z}_2 - k_2 z_2 = 0; \\
j = 2, & \quad m_2 \ddot{z}_2 + (c_2 + c_4) \dot{z}_2 + (k_2 + k_4) z_2 - c_2 \dot{z}_1 - k_2 z_1 - c_4 \dot{z}_3 - k_4 z_3 = 0; \\
j = 3, & \quad (m_3 + m_4 + m_N) \ddot{z}_3 + (c_3 + c_4) \dot{z}_3 + (k_3 + k_4) z_3 - c_4 \dot{z}_2 - k_4 z_2 - c_3 \dot{z}_1 - k_3 z_1 = F(t).
\end{aligned} \tag{4}$$

Based on differential equations of motion (3) and (4), corresponding energy models were created for the systems in question. By applying the First Principle of Power Distribution in a Mechanical System (1) one can move from a conventional dynamic analysis based on amplitudes of kinematic quantities to an energetic analysis of power distribution.

The energy model for the Human–Tool system, based on the model with two reduction points from the ISO 10068:2012 standard has the form:

$$\begin{aligned}
j = 1, & \quad m_1 \ddot{z}_1 \dot{z}_1 + (c_1 + c_2) \dot{z}_1^2 + (k_1 + k_2) z_1 \dot{z}_1 - c_2 \dot{z}_2 \dot{z}_1 - k_2 z_2 \dot{z}_1 = 0; \\
j = 2, & \quad (m_2 + m_N) \ddot{z}_2 \dot{z}_2 + c_2 \dot{z}_2^2 + k_2 z_2 \dot{z}_2 - c_2 \dot{z}_1 \dot{z}_2 - k_2 z_1 \dot{z}_2 = F(t) \dot{z}_2.
\end{aligned} \tag{5}$$

The energy model for the other Human–Tool system – Fig. 3b can be formulated as:

$$\begin{aligned}
j = 1, & \quad m_1 \ddot{z}_1 \dot{z}_1 + (c_1 + c_2 + c_3) \dot{z}_1^2 + (k_1 + k_2 + k_3) z_1 \dot{z}_1 - \\
& \quad - c_3 \dot{z}_3 \dot{z}_1 - k_3 z_3 \dot{z}_1 - c_2 \dot{z}_2 \dot{z}_1 - k_2 z_2 \dot{z}_1 = 0; \\
j = 2, & \quad m_2 \ddot{z}_2 \dot{z}_2 + (c_2 + c_4) \dot{z}_2^2 + (k_2 + k_4) z_2 \dot{z}_2 - \\
& \quad - c_2 \dot{z}_1 \dot{z}_2 - k_2 z_1 \dot{z}_2 - c_4 \dot{z}_3 \dot{z}_2 - k_4 z_3 \dot{z}_2 = 0; \\
j = 3, & \quad (m_3 + m_4 + m_N) \ddot{z}_3 \dot{z}_3 + (c_3 + c_4) \dot{z}_3^2 + (k_3 + k_4) z_3 \dot{z}_3 - \\
& \quad - c_4 \dot{z}_2 \dot{z}_3 - k_4 z_2 \dot{z}_3 - c_3 \dot{z}_1 \dot{z}_3 - k_3 z_1 \dot{z}_3 = F(t) \dot{z}_3.
\end{aligned} \tag{6}$$

Energy models for the Human–Tool systems were implemented in MATLAB/simulink software to calculate timelines of power of inertia, dissipation and elasticity. The resulting data was used to compare models in terms of power distribution.

4. An energy-based comparison of biomechanical Human–Tool systems

The biomechanical systems were subjected to a sinusoidal driving force $F(t)$ with the amplitude of 200 N. The analysis was conducted at following frequencies: 16Hz, 30Hz, 60Hz and 90Hz, assuming the mass of the tool m_N to be 6kg. Simulations were conducted for operation time t equal to 300 seconds, owing to the average deviation of the power value – below 1%. Simulations in the MATLAB/simulink software were implemented using integration time steps ranging from a maximum of 0.0001 to a minimum of 0.00001 second. The integration procedure ode113 (Adams) with a tolerance of 0.001 was used.

Figure 4 shows the impact of the frequency of driving impulses f on the percentage increase in the corresponding types of forces in for the model with three reduction points compared to values obtained for the model with two reduction points. The increase between the models is given by the following formula:

$$I_p = \frac{P_{3X(RMS),f}}{P_{2X(RMS),f}} \cdot 100\% \tag{7}$$

where:

$P_{3X(RMS),f}$ – RMS power of inertia, dissipation and elasticity for the Human–Tool system with three reduction points – power (RMS) in [W]:

- power of inertia expressed in [W]:

$$P_{3INE,f} = \sqrt{\frac{1}{t} \int_0^t [m_1 \ddot{z}_1 \dot{z}_1]^2 dt} + \sqrt{\frac{1}{t} \int_0^t [m_2 \ddot{z}_2 \dot{z}_2]^2 dt} + \sqrt{\frac{1}{t} \int_0^t [(m_3 + m_4 + m_N) \ddot{z}_3 \dot{z}_3]^2 dt};$$

- power of dissipation expressed in [W]:

$$P_{3LOS,f} = \sqrt{\frac{1}{t} \int_0^t [(c_1 + c_2 + c_3) \dot{z}_1^2]^2 dt} + \sqrt{\frac{1}{t} \int_0^t [(c_2 + c_4) \dot{z}_2^2]^2 dt} + \sqrt{\frac{1}{t} \int_0^t [(c_3 + c_4) \dot{z}_3^2]^2 dt};$$

- power of elasticity expressed in [W]:

$$P_{3ELA,f} = \sqrt{\frac{1}{t} \int_0^t [(k_1 + k_2 + k_3) z_1 \dot{z}_1]^2 dt} + \sqrt{\frac{1}{t} \int_0^t [(k_2 + k_4) z_2 \dot{z}_2]^2 dt} + \sqrt{\frac{1}{t} \int_0^t [(k_3 + k_4) z_3 \dot{z}_3]^2 dt};$$

$P_{2X(RMS),f}$ – RMS power of inertia, dissipation and elasticity for the Human–Tool system with two reduction points – power (RMS) in [W]:

- power of inertia expressed in [W]:

$$P_{2INE,f} = \sqrt{\frac{1}{t} \int_0^t [m_1 \ddot{z}_1 \dot{z}_1]^2 dt} + \sqrt{\frac{1}{t} \int_0^t [(m_2 + m_N) \ddot{z}_2 \dot{z}_2]^2 dt};$$

- power of dissipation expressed in [W]:

$$P_{2LOS,f} = \sqrt{\frac{1}{t} \int_0^t [(c_1 + c_2) \dot{z}_1^2]^2 dt} + \sqrt{\frac{1}{t} \int_0^t [c_2 \dot{z}_2^2]^2 dt};$$

- power of elasticity expressed in [W]:

$$P_{2ELA,f} = \sqrt{\frac{1}{t} \int_0^t [(k_1 + k_2) z_1 \dot{z}_1]^2 dt} + \sqrt{\frac{1}{t} \int_0^t [k_2 z_2 \dot{z}_2]^2 dt}.$$

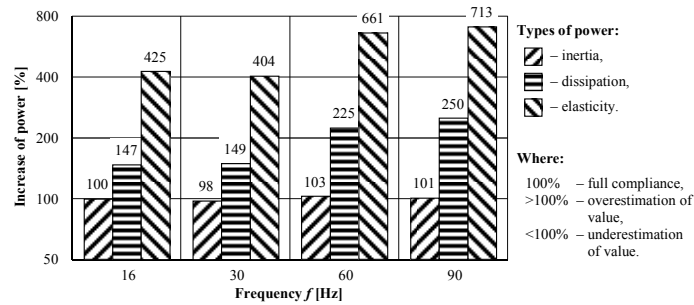


Figure 4. Impact of the frequency of driving impulses f on the increase in different types of powers

The comparison revealed that the contribution of the power of inertia in the human models from the ISO 10068:2012 standard is similar. Depending on the frequency of driving impulses, the maximum difference between the two models did not exceed 3%. Further analysis, however, showed much higher differences. The difference in the power of dissipation ranged from 47% to 150%. In the case of the power of elasticity, differences were much higher and ranged from 304% to as much as 613%. It should be noted that the difference between the models in terms of the power of dissipation and elasticity grows with increasing frequency. Assuming the maximum relative error of 30%, one cannot conclude that the results generated by the models are similar, except for the power of inertia.

Figure 5 depicts the influence of the frequency of driving impulses f on the percentage increase in the total power, which is the sum of the three kinds of power for the model with three reduction points in comparison with values obtained for the model with two reduction points, both from the ISO 10068:2012 standard. The percentage difference is given by the formula:

$$I_G = \frac{P_{3INE,f} + P_{3LOS,f} + P_{3ELA,f}}{P_{2INE,f} + P_{2LOS,f} + P_{2ELA,f}} \cdot 100\% \quad (8)$$

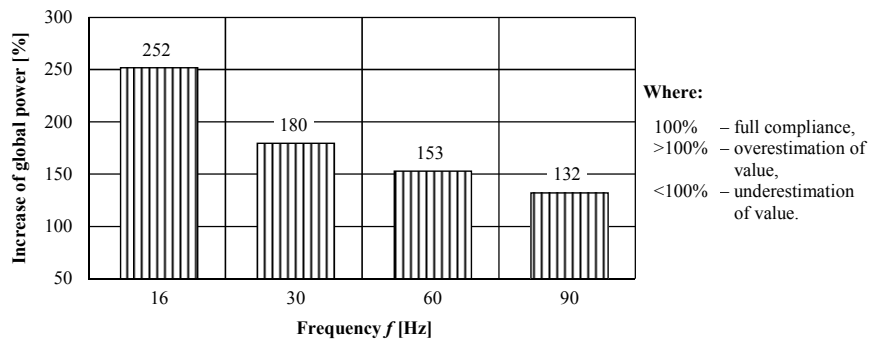


Figure 5. Influence of the frequency of driving impulses f on the increase in the total power

The results shown in Figure 5 indicate that the model with three reduction points always predicts higher total power compared to the reference model. What is more, the compatibility between the models increases significantly with increasing frequency f . An almost five-fold increase in accuracy can be observed for frequencies of 16 and 90 Hz, since the discrepancy between the models decreases from 152% to 32%. It is worth noting that even assuming the maximum relative error of 30% between the models, the corresponding results for each operating frequency of the Human–Tool system are never similar.

5. Summary

The comparison of human physical models specified in the ISO 10068:2012 standard revealed evident differences between them. The study showed a discrepancy between

the models considering the criterion of model similarity: the equality of different types of power. More importantly, the results indicated the biggest degree of similarity in the case of power of inertia, with a difference of no more than 3%. The results were much worse when it comes to the power of dissipation and elasticity, with difference ranging from 47% to 150% and from 304% to 613% respectively. The resulting differences obviously contributed to the degree of discrepancy in the total power, as shown in Fig. 5.

Moreover, the ISO 10068:2012-based model with three reduction points, shown in Fig. 3b, will undoubtedly provide a better protection for the operator of hand tools. This can be expected on account of a better power distribution predicted in the model, which is likely to increase the requirements for such tools. A more reliable verification of the models, would require energy measurements in a laboratory setting. For the time being it can only be concluded that the models we analysed are significantly different in their power distribution.

References

1. M.W. Dobry, *Optymalizacja przepływu energii w systemie Człowiek - Narzędzie - Podłoże (CNP)*, Rozprawa habilitacyjna, Seria „Rozprawy” nr 330, ISSN 0551-6528, Wydawnictwo Politechniki Poznańskiej, Poznań, 1998.
2. M.W. Dobry, *Energy diagnostics and assessment of dynamics of mechanical and biomechanics systems*, Machine Dynamics Problems, **25**(3/4) (2001), Warsaw University of Technology, Warsaw, 35-54.
3. M.W. Dobry, *Diagnostyka energetyczna systemów technicznych*, Inżynieria Diagnostyki Maszyn, Polskie Towarzystwo Diagnostyki Technicznej, Instytut Technologii Eksploatacji, Warszawa, Bydgoszcz, Radom, 2004, 314-339.
4. M.W. Dobry, *Podstawy diagnostyki energetycznej systemów mechanicznych i biomechanicznych*, Wydawnictwo Naukowe Instytutu Technologii Eksploatacji – PIB, Poznań-Radom 2012.
5. M.J. Griffin, *Handbook of Human Vibration*, Academic Press, London 1990.
6. A.M. Książek, *Analiza istniejących modeli biodynamicznych układu ręka – ramię pod kątem wibroizolacji człowieka – operatora od drgań emitowanych przez narzędzia ręczne*, Czasopismo Techniczne 2M/1996, Wydawnictwo Politechniki Krakowskiej, 87-114.
7. G. Meltzer, *A Vibration Model for the Human Hand-Arm-System*, Studies in Environmental Science, **13** (1981) 210-221.
8. D.D. Reynolds, W. Soedel, *Dynamic response of the hand-arm system to a sinusoidal input*. Journal of Sound and Vibration, **21**(3) (1972) 339-353.
9. ISO 10068:1998, Mechanical vibration and shock - Free, mechanical impedance of the human hand-arm system at the driving point.
10. ISO 10068:2012, Mechanical vibration and shock - Mechanical impedance of the human hand-arm system at the driving point.